88. Redetermination of the Crystal Structure of the 1,2,4,7-*anti*-Tetramethylbicyclo[2.2.1]heptan-2-yl Cation[1]) at 110 K

by **Thomas Laube***

Laboratorium für Organische Chemie, ETH-Zentrum, Universitätstrasse 16, CH-8092 Zürich

(7.II.94)

The structure of the 1,2,4,7-*anti*-tetramethylbicyclo[2.2.1]heptan-2-yl cation (**1**) was redetermined by X-ray crystal structure analysis of its Sb_2F_{11} salt at 110 K ($P2_1/c$, $R1 = 5.76\%$). The most important structural features of **1** are: C(1)–C(2) = 1.409(9), C(1)–C(6) = 1.710(8), and C(2)···C(6) = 2.113(9) Å and C(2)–C(1)–C(6) = 84.7(4)°. These results agree with those obtained earlier by other methods for the rapidly equilibrating, partially σ-delocalized 1,2-dimethylbicyclo[2.2.1]heptan-2-yl cation (**2**). The detailed experimental procedure for the preparation of crystalline $\mathbf{1}\cdot Sb_2F_{11}$ and the crystal selection and mounting are described.

The structure of the norborn-2-yl (= 8,9,10-trinorbornan-2-yl = bicyclo[2.2.1]heptan-2-yl) cation was the subject of a long debate in physical organic chemistry [1], and many methods were applied to investigate it (*e.g.* NMR [2a], IR [2b], and *ab initio* calculations [2c]). Crystal-structure analysis, however, was hardly used because of the difficulties of growing suitable single crystals[2]). We report in this work the results of a more precise redetermination of the up to now only crystal structure of the salt of a purely alkyl-substituted norborn-2-yl cation [4], *i.e.*, of $\mathbf{1}\cdot Sb_2F_{11}$, at the lowest temperature available to us (110 K). The crystal structure of a better stabilized 2-methoxynorborn-2-yl cation was determined by *Montgomery et al.* [5]. The ion **1** is electronically related to

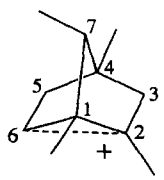

1

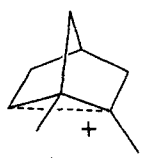

2

the 1,2-dimethylbicyclo[2.2.1]heptan-2-yl cation (**2**), because the additional Me groups at C(4) and C(7) are expected to have only minimal electronic influence. The ion **2** and the unsubstituted parent ion were also thoroughly investigated [6], and **2** was found to be equilibrating and partially σ-delocalized, in contrast to the unsubstituted ion.

---

[1]) Formerly called '1,2,4,7-*anti*-tetramethyl-2-norbornyl cation'.

[2]) To our knowledge, the earliest hint to the existence of crystalline norborn-2-yl salts was given by *Olah* [3a]. Crystallization and attempted crystal-structure analyses were reported by *Dinnocenzo* [3b].

Results. – The synthesis of **1** (see *Scheme 1*) follows a procedure of *Coxon* and *Steel* [7] and starts with commercially available fenchol (**3**), which is tosylated (→ **4**) and, in a formolysis, converted into a mixture of fenchyl formiates (**5**) and isofenchyl formiates (**6**).

Scheme 1

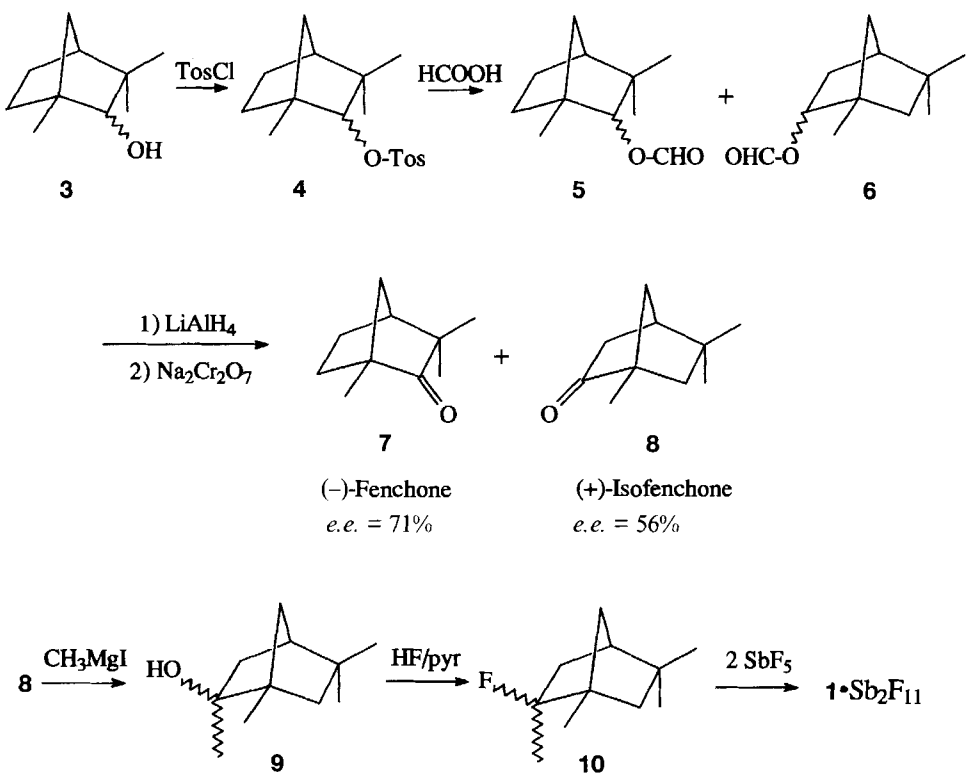

The formyl groups are cleaved off reductively, and the resulting mixture of alcohols is oxidized to a mixture of fenchone (**7**) and isofenchone (**8**). The loss of optical purity is not important (see below). Pure **8** is converted into the tertiary alcohol **9**, from which the fluoride **10** is synthesized according to *Olah et al.* [8]. The reaction of **10** with 2 equiv. of SbF_5 yields upon recrystallization from CH_2Cl_2 crystalline $\mathbf{1} \cdot Sb_2F_{11}$ (racemic; space group $P2_1/c$), which is used for the crystal-structure analysis (see *Exper. Part*). A ^{1}H-NMR spectrum of the crystals of $\mathbf{1} \cdot Sb_2F_{11}$ dissolved in CD_2Cl_2 is dominated by two broad peaks indicating rapid exchange in solution. The spectrum is similar to that of **1** (and isomers) in FSO_3H/SO_2ClF obtained by *Sorensen* and coworkers [9].

The result of the crystal-structure analysis (*Figs. 1* and *2*) is not very different from the already published structure at 193 K, but it is more precise (110 K: $R1 = 5.76\%$; 193 K: $R = 8.0\%$ [4a]). The most important differences occur around the atoms C(1), C(2), and C(6). The bonds C(1)–C(2) (1.409(9) Å) and C(1)–C(6) (1.710(8) Å) are *ca.* 0.03 Å shorter and the angle C(2)–C(1)–C(6) (84.7(4)°) is *ca.* 3° larger than previously reported.

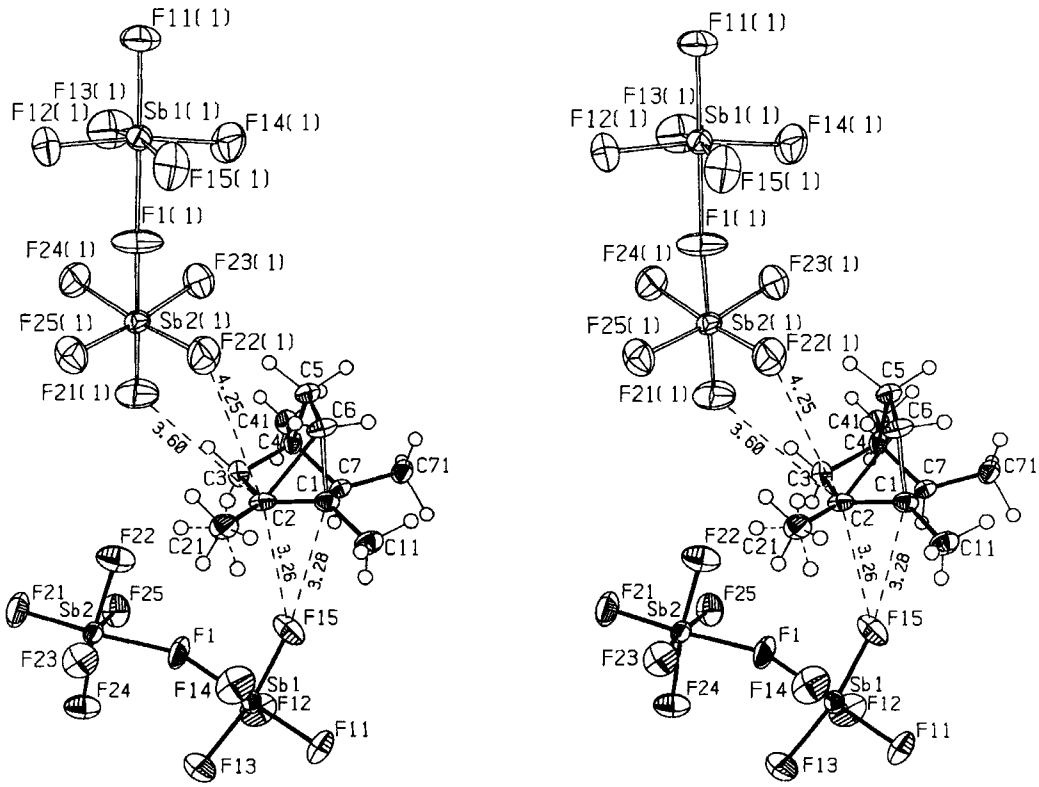

Fig. 1. *ORTEP stereodrawing of the crystal structure of* **1** · Sb_2F_{11}. The atoms of the symmetry-related anion are drawn as empty ellipsoids, and their labels are followed by the symmetry-operation number (see legend to *Fig. 3*). The displacement ellipsoids are drawn at the 50% probability level, the H-atoms are represented by spheres with a radius of 0.1 Å. For C(21), two partially populated sets of methyl H-atoms are refined (populations and bond types: 0.6 = solid bonds, 0.4 = dashed bonds). Distances are given in Å.

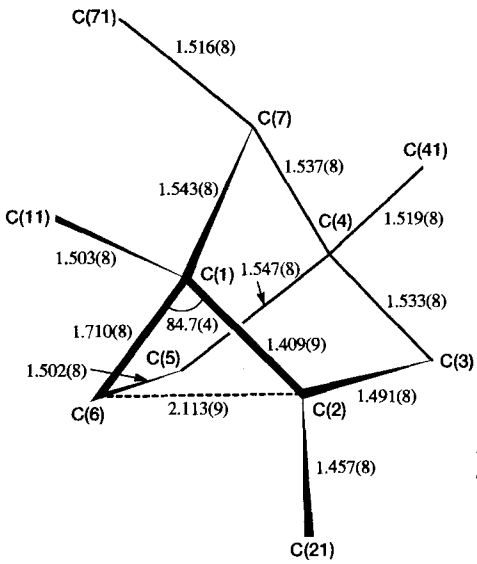

Fig. 2. *Selected bond lengths* [Å] *and angles* [°] *in the crystal structure of* **1**

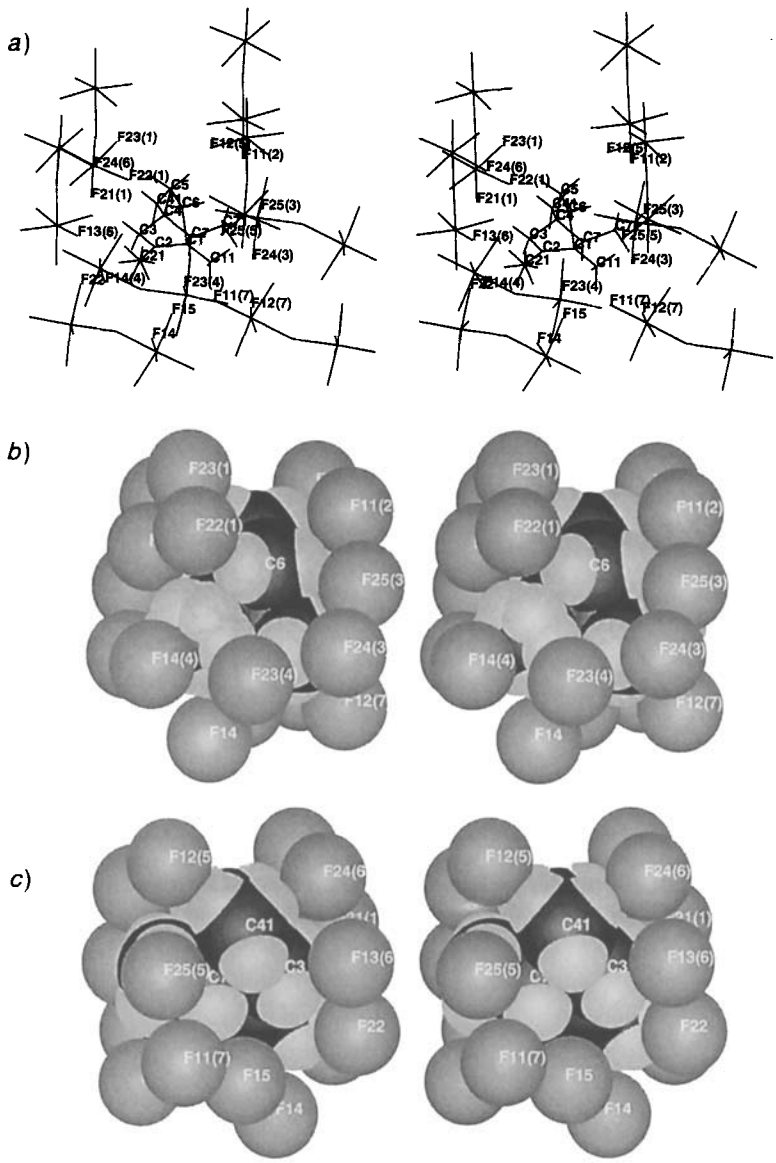

Fig. 3. *Stereodiagram of the anion surrounding of* **1** *in the crystal structure of* $\mathbf{1}\cdot Sb_2F_{11}$. The symmetry operations (given in parentheses) are as follows: (1) $-x+1, y-1/2, -z+3/2$; (2) $x, -y+1/2, z+1/2$; (3) $x, y-1, z$; (4) $-x+1, -y+1, -z+1$; (5) $-x+2, y-1/2, -z+3/2$; (6) $x, -y+3/2, z+1/2$; (7) $-x+2, -y+1, -z+1$. *a*) Wire-frame diagram of cation **1** with its 8 nearest counterions (the F-atoms with H···F ≤ 2.87 Å, *i.e.* sum of the *van der Waals* radii +0.2 Å, are labelled). *b*) Space-filling representation of cation **1** and the nearest F-atoms from counterions (view direction as above). *c*) The atoms cluster shown in *Fig. 3b* rotated by 180° around a vertical axis. H···F distances less than 2.67 Å: H(3*n*)···F(21)(1) = 2.49, H(5*n*)···F(23)(1) = 2.64, H(5*x*)···F(11)(2) = 2.60, H(6*x*)···F(11)(2) = 2.65, H(7)···F(11)(7) = 2.64, H(111)···F(25)(3) = 2.63, H(211)···F(22) = 2.60, H(213)···F(14) = 2.58, H(214)···F(23)(4) = 2.56, H(216)···F(21)(1) = 2.60, H(412)···F(12)(5) = 2.34, H(711)···F(25)(5) = 2.57, H(712)···F(11)(2) = 2.53 Å.

The C-atom C(2) is planar, while C(1) is pyramidal, if the C(1)–C(6) bond is ignored (distances Δ from the plane through the three bond partners: $\Delta_{C(2)} = 0.002(6)$, $\Delta_{C(1)} = -0.257(6)$ Å). The Me H-atoms at C(21) are rotationally disordered, as often observed with Me groups at sp^2 C-atoms; many of the other H-atoms can be freely refined on reasonable positions. Thermal-motion analysis based on a rigid-body model does not account well for the observed displacement parameters of **1** ($R = 17.1\%$, see *Exper. Part*). Some cation-anion contacts are shorter at 110 K (*e.g.* C(2)···F(22)(1) 4.25 and C(6)···F(22)(1) 3.62 Å) than at 193 K (4.33 and 3.73 Å, resp.). The cation **1** has approximate *van der Waals* contact to eight anions (see *Fig. 3*), and the packing pattern of $\mathbf{1} \cdot Sb_2F_{11}$ resembles a distorted CsCl lattice (see *Supplementary Material*). Electron- and difference-density contour diagrams (*Fig. 4* and *Supplementary Material*) show that the cation **1** is located in a region of elevated diffuse 'background' electron density (highest difference-density peaks: *ca.* 0.9 $eÅ^{-3}$).

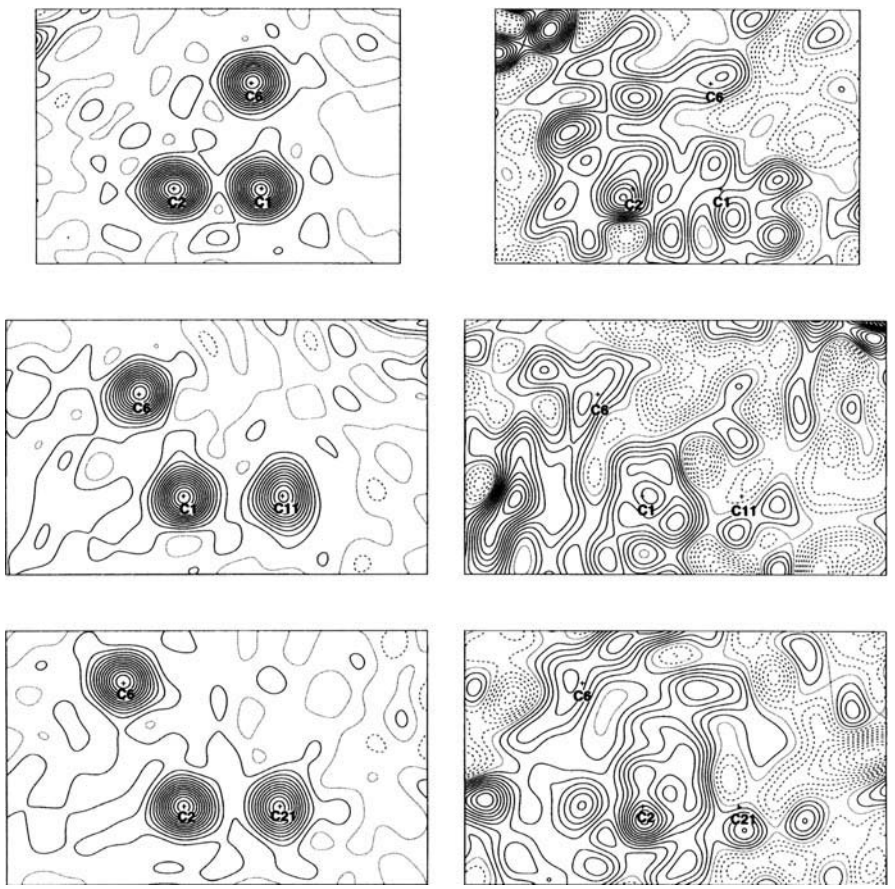

Fig. 4. *Electron-density* (F_{obs}; left) *and difference-density* ($F_{obs} - F_{calc}$; right) *maps of three planes of* **1**. The density differences between two contour lines are 1.0 $eÅ^{-3}$ for the electron density and 0.1 $eÅ^{-3}$ for the difference density. Positive density: solid lines; zero: dotted line; negative: dashed lines.

Attempts to connect the difference-density maxima to another orientation of **1** or another cation failed (see *Supplementary Material*), but two peaks could be refined as additional C-atoms with free site occupation factors (0.12 and 0.07). The most severe disagreement between observed and calculated electron density occurs around the Sb-atoms (see *Supplementary Material*), and a slight disorder of the anion is indicated also by the high anisotropy of the probability density function of the central F-atom F(1) (ratio of the largest to the smallest eigenvalue of the displacement parameters: 6.7, $U_{eq}(F(1)) = 0.061(2)$ Å^2; for comparison: in the more precise structure of the (*tert*-butyl)Sb_2F_{11} salt [10] at 193 K, this ratio for F(1) is only 2.0, and $U_{eq}(F(1)) = 0.043(1)$ Å^2). The difference-density contour diagrams in the anion region does not yield hints for additional minor, unrecognized orientations of the anion, but unresolvable disorder is possible.

Discussion. – *Formation of* **1**. The formation of **1** *via* a sequence of rearrangements starting from cation **11**, which must be formed directly upon F-abstraction from **10**, was not experimentally investigated, but the shortest path (in terms of number of intermediate ions) using known rearrangement steps is shown in *Scheme 2*. It was obtained using a program similar to that of *Johnson* and *Collins* [11]. It is probable, that many other intermediate ions exist, and even the fact, that **1** · Sb_2F_{11} crystallizes from solution does not mean, that **1** is predominant in solution (at least its *Wagner-Meerwein* isomer **16** may be present in comparable amounts [9], see *Scheme 2*).

Scheme 2

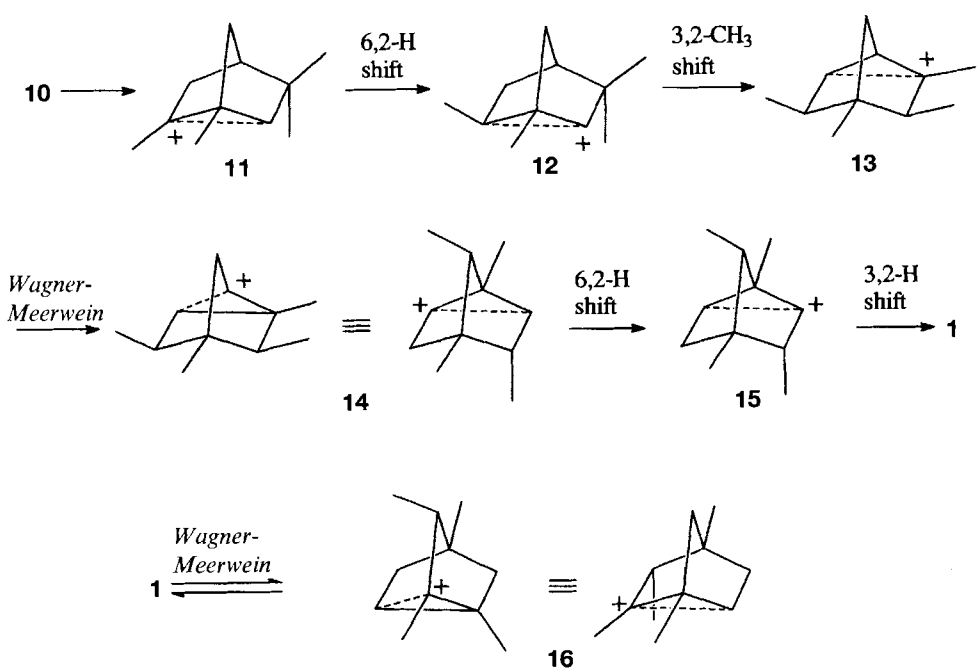

Structure of **1**. The structure of **1** deviates strongly from that of a neutral norbornane derivative [4a] [12]. The following deviations of bond lengths and angles in **1** from suitable reference values [13] are considered to be important. A normal C_{sp^2}–$C_{sp^3}(C_{sp^3})_3$ bond has a length of 1.522(1) Å, and thus C(2)–C(1) is shortened by 0.113(9) Å; C(2)–C(21) is shortened by 0.046(8) Å (normal C_{sp^2}–Me bond: 1.503(1) Å), C(1)–C(11) is shortened by 0.031(8) Å (normal $(C_{sp^3})_3C_{sp^3}$–Me bond: 1.534(1) Å), C(2)–C(3) is only insignificantly shortened by 0.011(8) Å (normal C_{sp^2}–$CH_2(C_{sp^3})$ bond: 1.502(1) Å), and C(1)–C(6) is lengthened by 0.172(8) Å (normal $(C_{sp^3})_3C_{sp^3}$–$CH_2(C_{sp^3})$ bond: 1.538 (1) Å). In terms of the MO description, these features are the result of the interaction of the empty p orbital at C(2) ($p_{C(2)}$) with the filled bond orbitals in the neighbourhood. The interaction with the ideally aligned $\sigma_{C(1)-C(6)}$ orbital (torsion angle between the symmetry axis of $p_{C(2)}$ and C(1)–C(6): −7°) leads to an unsymmetrical 3-center-2-electron bond involving C(2), C(1), and C(6). Simultaneously, $p_{C(2)}$ is also interacting with the C(21) Me group leading to C–H hyperconjugation (probably somewhat weaker than in the *tert*-butyl cation where the average C^+–Me bond lengths is 1.442(5) Å [10]). The interaction between $p_{C(2)}$ and the $\sigma_{C(3)-H(3x)}$ orbital can only be inferred from the nearly ideal torsion angle between them (+12°), while the $p_{C(2)}/\sigma_{C(3)-H(3n)}$ interaction must be worse because of the torsion angle of −46° (in agreement with the fact that the 3,2-*exo*-H shift in norborn-2-yl cations is much faster than the 3,2-*endo*-H shift [14]). The orbitals involved in the postulated electronic effects are depicted in *Fig. 5*.

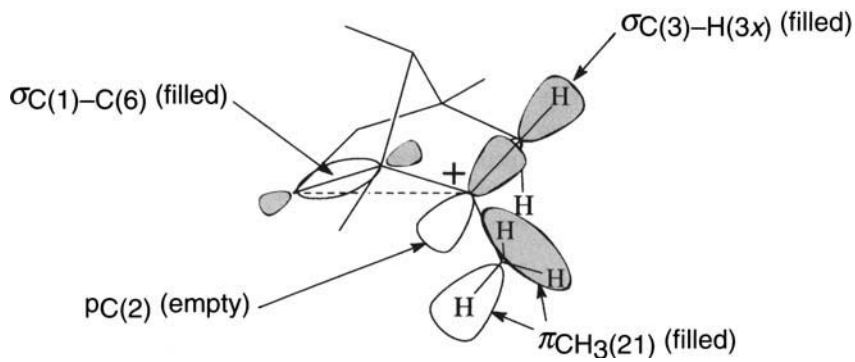

Fig. 5. *Orbital description of the charge delocalization in* **1**

Packing of **1** · Sb_2F_{11}. *Fig. 3* shows that **1** is in *van der Waals* contact to many F-atoms from totally eight counterions, and *Fig. 1* shows that F(15) has practically the same distances to C(2) (3.260(8) Å) and to C(1) (3.277(8) Å), *i.e.* both are *ca.* 0.1 Å greater than the sum of the *van der Waals* radii (3.17 Å). While these two distances do not change if compared with the structure at 193 K, contacts to the anion generated by symmetry operation (1) (see legend of *Fig. 3*) are *ca.* 0.1 Å shorter in the low-temperature structure presented here (*e.g.* C(2)···F(22)(1) = 4.25 and C(6)···F(22)(1) = 3.62 Å) than at 193 K (see *Results*). It is striking that the vector from F(22)(1) to C(6) (in crystal coordinates: $(0.3127, -0.0079, -0.0420)^T$) is practically parallel to the *a* axis which is the axis with the highest temperature dependence[3]) (see *Exper. Part* and *Supplementary Material*, fig. S8–

[3]) For a discussion of other examples of anisotropic thermal expansion, see [15].

S12). Thus, it may be possible that the strong shrinking of the crystal in this direction upon cooling is due to a reduction of a movement of C(6) along the path leading to the *Wagner-Meerwein* isomer **16** in the crystal. The fact that the angle C(2)–C(1)–C(6) is *ca.* 3° larger at 110 K than at 193 K also indicates that the previously published high-temperature structure was perhaps influenced by such an internal motion. An earlier estimation [4c] of the possible coordinate error for C(6) in the structure at 193 K yielded 0.07 Å and a resulting correction of C(2)–C(1)–C(6) by 2.3°, in good agreement with the now determined structure at 110 K.

Consideration of Disorder of **1**. The structure of $\mathbf{1}\cdot Sb_2F_{11}$ contains two hints that **1** is not perfectly ordered: the electron-density background in the cation region and the poor agreement of observed and calculated U values (which may be a consequence of the background density or of a failure of the rigid-body model). The mediocre $R1$ value of 5.76% may be mainly due to the disagreement of computed and observed electron density in the anion region. On the other hand, the fact that most H-atoms could be refined freely to reasonable positions is an indication that the assumed disorder is not severe. Because of the lack of a refinable second orientation or another cation, we can only estimate the possible positional errors of the C-atoms due to unresolvable disorder. If the highest difference-density peak (see *Exper. Part*) is treated as a C-atom, a site-occupation factor of 0.12 is obtained. Such a peak can cause positional errors of up to *ca.* 0.03 Å for the C-atoms in the structure of **1** [4c]. Such an error is too small to interpret the structure of **1** as a superposition of cations with a structure similar to a neutral norbornane derivative[4]).

Finally, the residual density peaks may also be due to an imperfect absorption correction (see *Exper. Part*). To the extent that the error in absorption correction takes the form of a second-order tensor, it may be absorbed into the displacement parameters. The remaining errors take the form of higher-order tensor, and may very well lead to uninterpretable difference densities, especially in the neighbourhood of heavy atoms, *i.e.* the residual electron density can be interpreted in terms of disorder, insufficient absorption correction, or both. The data do not allow to distinguish between the various possibilities[5]).

Conclusion. – The crystal-structure analysis of $\mathbf{1}\cdot Sb_2F_{11}$ shows that the cation is strongly distorted if compared with a neutral norbornane derivative. The structural deformations in **1** are in agreement with the assumption of interactions of the filled $\sigma_{C(1)-C(6)}$ and $\pi_{CH_3(21)}$ orbitals with the empty p orbital at C(2) (σ participation and C–H hyperconjugation). Similar results were obtained earlier by other methods [6] for the rapidly equilibrating, partially σ-delocalized ion **2**.

Experimental Part

General. All solvents used for the carbocation experiments were distilled over P_2O_5 and stored under Ar.

Separation of the Fenchone/Isofenchone (**7**/**8**) *Mixture.* A mixture **7**/**8** 55:45 (81.3 g; obtained according to *Coxon* and *Steel* [7]) was separated by distillation at 5.5 mbar for 100 h in a 'Spaltrohr' column (*Fischer*) with *ca.* 90 theoretical plates (effective reflux ratio 250:1 to 500:1): 32.7 g of **7** (b.p. 68–70°; GC: 97% pure; $\alpha_D^{20} = -43.964°$ (pure substance, 10 cm); *e.e.* = 71%) and 31.6 g of **8** (b.p. 72–73°; GC: 99% pure; $\alpha_D^{20} = +4.418°$ (pure substance, 10 cm); *e.e.* = 56%) as colourless liquids.

---

[4]) This superposition is shown in [4b], Fig. 13.

[5]) I thank a referee for this clarification.

1,2,5,5-Tetramethylbicyclo[2.2.1]heptan-2-ol (**9**). A soln. of **8** (4.0 g, 26.3 mmol) in THF (15 ml) was added to a freshly prepared soln. of MeMgI (261 mmol) in Et_2O (85 ml). The mixture was refluxed for 4 h and hydrolyzed by pouring into ice/NH_4Cl soln. (800 ml). After workup and drying (Na_2SO_4), the product was reacted for a 2nd time under identical conditions with MeMgI because of the presence of a small amount of unreacted **8** according to IR spectroscopy. The product of the 2nd reaction was bulb-to-bulb distilled (100° (air bath)/0.01 mbar): 3.68 g (83%). Slightly yellow oil. ^{1}H-NMR (90 MHz, $CDCl_3$): 0.98, 1.03, 1.08, 1.23 (4*s*, 12 H); 0.7–2.0 (*m*, 8 H).

2-Fluoro-1,2,5,5-tetramethylbicyclo[2.2.1]heptane (**10**). A soln. of **9** (3.5 g) in pentane (40 ml) was added to a mixture of HF/pyridine (*Fluka* or *Aldrich*; 25 ml) and pentane (10 ml) at 0° in a polyethylene bottle [8]. The mixture was vigorously stirred for 2 h at 0° and then poured into ice/H_2O (200 ml) and pentane (200 ml). The org. phase was washed rapidly with H_2O, dil. $NaHCO_3$ soln., and again H_2O and dried (Na_2SO_4) at 0°. After removal of *ca.* 95% of the solvent at r.t., the raw product was distilled in a high-vacuum (h.v.) line into a *Schlenk* tube: 3.08 g of **10**. Colourless oil which is stored in a freezer. ^{1}H-NMR (300 MHz, $CDCl_3$): presence of small amounts of other isomers probably formed during fluorination; major isomer: 0.934 (*s*, 3 H); 1.013 (*s*, 3 H); 1.043 (*s*, 3 H); 1.332 (*d*, J = 22.8, 3 H); 1.779 (*ddd*, J = 38, 13.5, 4.8, 1 H); 1.936 (*ddd*, J = 18, 13.5, 4.2, 1 H); 0.7–2.0 (*m*, 5 H); minor isomer (identifiable signals): 1.296 (*d*, J = 22.9, 3 H); 2.075 (*ddd*, J = 23, 14.3, 4.3, 1 H); see *Supplementary Material*, fig. S24.

1,2,4,7-anti-Tetramethylbicyclo[2.2.1]heptan-2-ylium Undecafluorodiantimonate(V) (**1**·Sb_2F_{11}). To a soln. of **10** (0.57 g, 3.35 mmol) in $CFCl_3$ (45 ml; see *Fig. 6*, reaction vessel, compartment A) was added at −80° under Ar a soln. of SbF_5 (1.50 g, 6.92 mmol; 2.07 equiv.) in CCl_2FCClF_2 (10 ml) from the PTFE (poly(tetrafluoroethene))

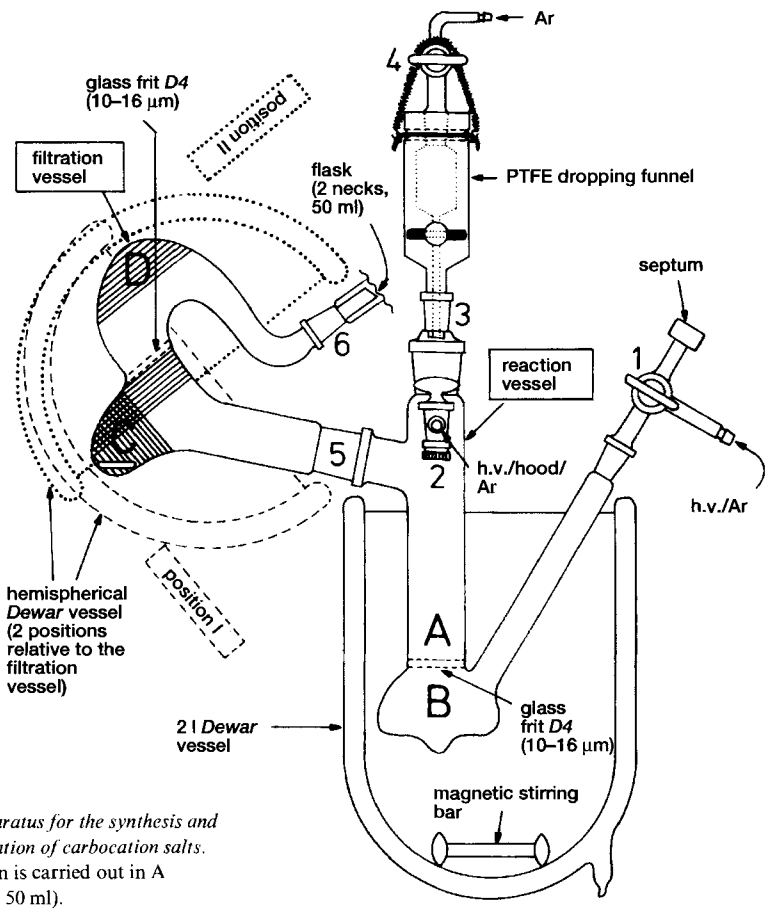

Fig. 6. *Apparatus for the synthesis and recrystallization of carbocation salts.* The reaction is carried out in A (volume *ca.* 50 ml).

dropping funnel (volume 10 ml; slight Ar over-pressure). After bubbling Ar (from B) for 1 h through the mixture (the Ar outlet is stopcock 2), the PTFE dropping funnel was removed and a septum placed on joint 3, and for the filtration of the yellow, slightly turbid mixture, Ar over-pressure (from stopcock 2) and slight vacuum (through stopcock 1) were applied. The mother liquor collected in B was then removed with a long needle through the septum on stopcock 1 by Ar over-pressure. The resulting filter cake on the frit (yellow to orange, glassy) was dried in A at −80 to −45° at $< 10^{-2}$ mbar (h.v. applied through stopcocks 1 and 2) for *ca.* 2 h. During this time, the filter cake becomes colourless, hard, and nontransparent. After refilling the apparatus with Ar (the reaction vessel was permanently cooled), the filter cake was coarsely powdered at −80° with a long spatula through joint 3 (flushed with Ar). The whole apparatus was quickly turned to the left by *ca.* 100 degrees so that the filtration vessel could be cooled to −80° in a magnetically stirred cooling bath in a hemispherical *Dewar* vessel, and the raw powdered salt was very quickly transferred with the spatula from A into the precooled compartment C. The reaction vessel on joint 5 was replaced by an adapter with a 3-way stopcock with a septum and an Ar inlet. The salt was cooled to −105° or lower (filtration apparatus in position I) and CH_2Cl_2 (20 ml) very slowly added with a syringe through the 3-way stopcock on joint 5 into C. To avoid decomposition, the salt should be dissolved in melting CH_2Cl_2. The yellow to orange soln. was warmed to −60°, stirred for 10 min, and filtered at −60° into D by turning the filtration apparatus into position II. A small residue of the salt remained on the frit. The clear filtrate was collected and then quickly poured into the precooled 50-ml 2-neck flask (with an adapter with a 3-way stopcock with septum on its second joint) connected to the filtration vessel at joint 6. The flask was then disconnected from joint 6, stoppered, and stored on dry ice. The crystal growth began after a few h and was usually complete within 12 h. The mother liquor was removed with a syringe at −80°, and the colourless to slightly yellow crystals (somewhat intergrown plates, length up to 2 mm) were washed with CH_2Cl_2 (2 ml) and dried between −80 and −60° (never higher) under h.v.

Crystal Selection and Mounting and X-Ray Measurements. The dried crystals were examined and mounted under dry N_2 on a self-constructed cryostage[6]) (*Fig. 7*). After cooling the stage to −60°, the cold flask with the dried crystals was placed in one of the cooled jacketed steel beakers of the cryostage. The crystals were placed on a slide

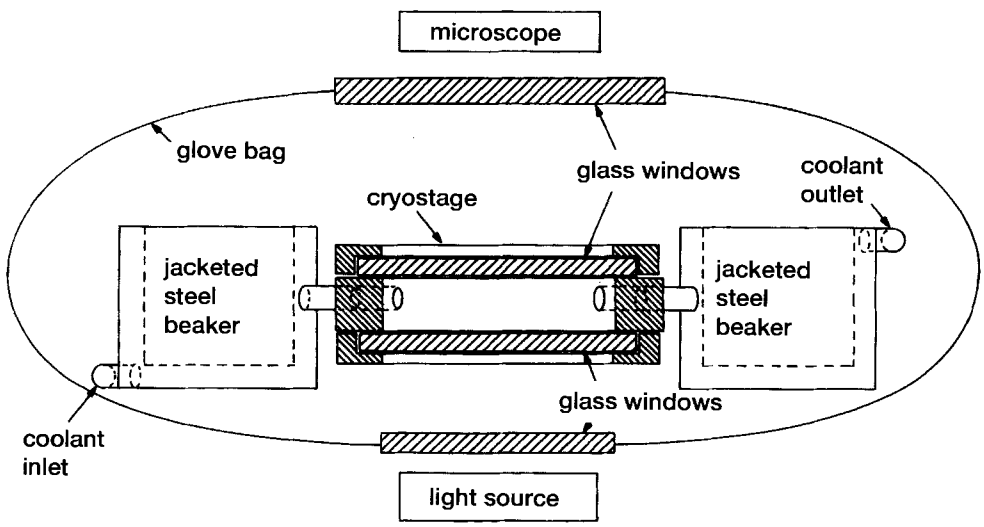

Fig. 7. *Schematic drawing of the cryostage.* The whole stage with the beakers is made from stainless steel (welded; gas-tight) and cooled with circulating MeOH (cryostat). The stage is situated between two glass windows (in a metal frame) in a medium-sized glove bag. The N_2 in the glove bag is circulating through a tower with molecular sieve as drying agent. All sealings of the glove bag (glass windows, coolant inlet and outlet, drying tower) are gas-tight. The working area on the cooled glass window of the cryostage has a diameter of 10 cm. The metal parts of the cryostage are thermally insulated.

[6]) Many other techniques for the handling of crystals at low temperatures are described in [16]. For another, newer technique, see [17].

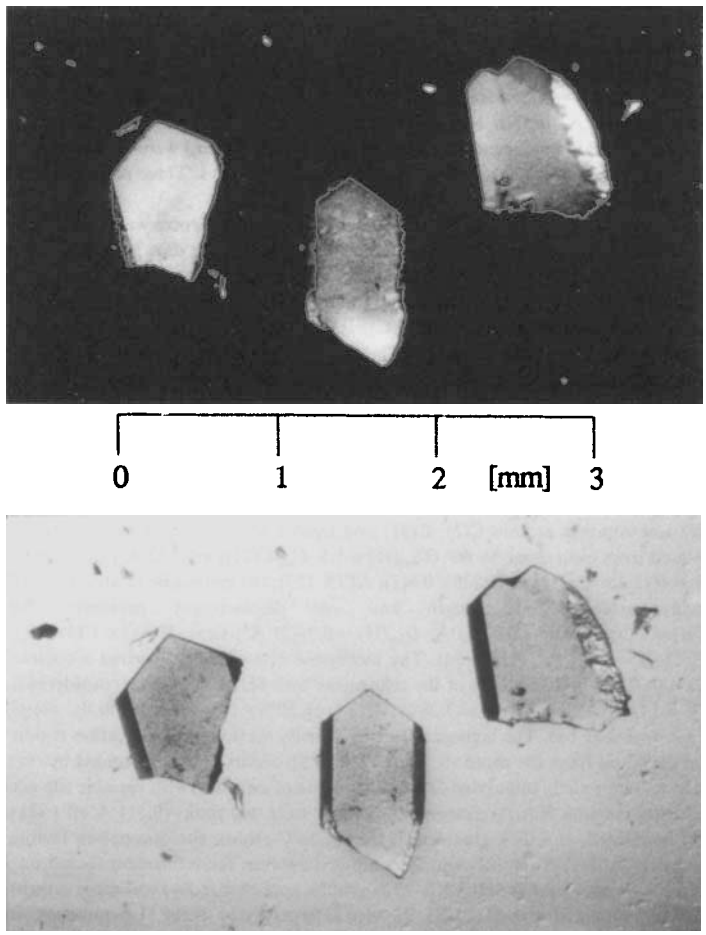

Fig. 8. *Photographs of crystals of* **1**·Sb_2F_{11} *at* $-60°$ *in a dry* N_2 *atmosphere under polarized light* (top: crossed polarizers; bottom: parallel polarizers)

with a depression filled with a perfluorinated polyether of low viscosity (*Galden D05*; *Montedison*, Milan, Italy). Suitable crystals (see *Fig. 8*) were selected and cut (if necessary) under a binocular microscope (with photo equipment) using polarized light, mounted on a glass fiber with a perfluorinated polyether with a suitable pour point (*Aflunox 606*; *PCR*, Gainesville, Florida) as adhesive [18] and stored in a rack in the second steel beaker (the crystals were kept at low temp. and under inert gas during all operations). The rack with the mounted crystals was then transferred into a large *Dewar* vessel, where it was stored in a cold N_2 atmosphere (*ca.* $-100°$).

The X-ray measurements were carried out on an *Enraf-Nonius-CAD4* diffractometer (MoK_α radiation with $\lambda = 0.71069$ Å, graphite monochromator). The crystal (approximate size in mm: $0.7 \times 0.5 \times 0.2$) was mounted on the diffractometer at $-100°$ and slowly cooled in seven steps to $-163°$. There was no hint from the changes of the cell data of two different crystals to a phase transition in this temp. range[7]) (see *Supplementary Material*, figs.

[7]) Upon slow warming of the crystals in *Galden D05* on the cryostage, the following observations were made: at $-30°$, the crystals were significantly softer than at $-60°$, and between -20 and $-15°$, a phase transition (accompanied with a vivid formation of stripe patterns visible under polarized light) occurred which shattered the crystals. At 0°, the shattered crystals were plastic and sticky, but a chemical decomposition (*e.g.* gas evolution, change of color *etc.*) was optically not detectable, not even at 20°.

S8–S12). The rounded average linear thermal expansion coefficients along the direct axes in this temperature range were $\alpha_a = 150 \cdot 10^{-6}\ K^{-1}$, $\alpha_b = 60 \cdot 10^{-6}\ K^{-1}$, $\alpha_c = 70 \cdot 10^{-6}\ K^{-1}$, and the average volume expansion coefficient is $\beta = 280 \cdot 10^{-6}\ K^{-1}$. The directions of the principal axes of the thermal expansion tensor were not determined. The final monoclinic cell data at −163° were $a = 11.247(3)$, $b = 10.619(5)$, $c = 14.969(3)$ Å, $\beta = 94.72(2)$ deg, $V = 1782(1)$ Å^3, space group $P2_1/c$ (No. 14); $\mu = 3.13$ mm^{-1}; $M_w(C_{11}H_{19}Sb_2F_{11})$ 603.754, $Z = 4$, $\rho_x = 2.251$ g cm^{-3}, $F_{000} = 1144$. A total of 5195 independent reflections (3791 with $I > 2\sigma_I$) were measured with Ω-2ϑ scans up to $\vartheta = 30°$ ($0 \leqslant h \leqslant 15$, $0 \leqslant k \leqslant 14$, $-20 \leqslant l \leqslant 20$), maximal scan time 150 s. Three repeatedly measured monitor reflections (404, 216, 242) showed practically no decay.

X-Ray Crystal-Structure Determination of **1**·Sb_2F_{11}. The systematic absences were controlled with a program [19] which plots the intensities in arbitrary planes in the reciprocal space. The data reduction was carried out with DIFDAT [20] from the Xtal 3.2 [21] system, an empirical absorption correction (with 36 scans of the reflection 150, which had $\chi \approx 90°$; minimum 1.0091, maximum 2.1789) was applied with ABSCAL [22][8], and a HKLF file for the SHELX programs [23] [24] was generated with LISTFC [25]. The positions of the Sb-, F-, and C-atoms of **1**·Sb_2F_{11} were determined with the *Patterson* option of SHELXS-86 [23] using the data up to $\vartheta = 25°$; they were practically identical with the already published coordinates. The structure was first refined upon F^2 with SHELXL-93 [24]. After several cycles of isotropic and anisotropic refinement (full matrix; $w = 1/[\sigma_{F_{obs}}{}^2 + (0.0987\ P)^2]$ with $P = (\max(F_{obs}{}^2,0) + 2\ F_{calc}{}^2)/3$; extinction parameter: 0.0037(5)), all H's with the exception of one in each case at C(21), C(3), and C(5) could be located in the difference-density maps on reasonable positions. Treatment of other peaks of the soln. obtained by SHELXS-86 as C- or F-atoms did not yield new atomic positions upon refinement. After several attempts, the following constraints were applied for the H-atoms: the C(21) H-atoms were allowed to ride on C(21) with free rotation around C(2)–C(21) and treated as rotationally disordered assuming two Me conformations rotated from each other by 60° ($U_{iso}(H) = 1.5 \cdot U_{eq}(C(21)) = 0.052$ Å^2; site-occupation factors for H(211) to H(213): 0.4(1); for H(214) to H(216): 0.6(1); AFIX 127); the methylene H-atoms at C(3) and C(5) were riding with one variable C–H length and one displacement parameter for each CH_2 group (C(3)–H(3*n*) = C(3)–H(3*x*) = 0.93(5) Å, $U_{iso}(H) = 0.04(2)$ Å^2; C(5)–H(5*n*) = C(5)–H(5*x*) = 1.10(4) Å, $U_{iso}(H) = 1.2 \cdot U_{eq}(C(5)) = 0.031$ Å^2; AFIX 24). The methylene H-atoms at C(6) had a common displacement parameter $U_{iso}(H) = 0.02(1)$ Å^2. The results of the refinement with SHELXL-93 are considered as final ($I > 2\sigma_I$: $R1 = 5.76\%$, $wR2 = 14.40\%$; all data: $R1 = 7.28\%$, $wR2 = 16.50\%$); they are listed in the *Supplementary Material* and used for the drawings 1–3. The highest difference-density maximum in the cation region was 0.92 eÅ^{-3} (root mean-square deviation from the mean: 0.31 eÅ^{-3}). The Sb-atoms were surrounded by maxima up to 2.13 eÅ^{-3}. An attempt to refine partially populated C-atoms (because of disorder) with variable site-occupation factors on all difference-density maxima failed (refinement unstable); only two peaks (0.511 Å off C(3) and 0.515 Å off C(71), resp.) could be refined, and they obtained, if treated as C-atoms, site-occupation factors of 0.12(4) and 0.07(4). To obtain electron- and difference-density contour diagrams, the refinement (based on F^2; full matrix; $w = 1/\sigma_{F_{obs}}{}^2$; the same weights used in SHELXL-93 cannot be applied directly) was repeated with CRYLSQ [26] where the H-parameters obtained with SHELXL-93 were kept invariant (if the H-parameters were also refined, some of them were not as stable as in SHELXL-93). An extinction correction according to *Becker* and *Coppens* [27] (*Gaussian* distribution) was applied and refined in the last cycles of the refinement with CRYLSQ ($g = 0.44(4)$; final R values: $R = 5.8\%$ (using $|F|$), $wR = 14.5\%$ (using $|F^2|$)). The structures obtained by the SHELXL-93 and the CRYLSQ refinements were not significantly different. The maxima of the difference-density function had slightly higher values than after the SHELXL-93 refinement (up to 1.17 eÅ^{-3} in the cation region, 2.31 eÅ^{-3} around the Sb-atoms, 2.66 eÅ^{-3} at Sb(2)). The electron- and difference-density contour maps for 29 planes (see *Fig. 4* and *Supplementary Material*, figs. S13–S20) were generated with the program sequence FOURR [28], SLANT [29], CONTRS [30], PREVUE [31], PLOTX [32]; the density functions were analyzed with PEKPIK [33]. *Fig. 1* was generated with ORTEP [34], *Fig. 3* with *SYBYL*® 6.0 [35]. Most geometry calculations and the preparation of most tables in the supplementary material were carried out with a modified version of PARST88 [36]. A thermal-motion analysis of **1** with THMA11 [37] (using the σ_U values for weights; assuming a rigid body) gave a weighted R for all U's of 17.1% and for the diagonal U's of 14.8%. The roots of the eigenvalues of the **L** and T tensors were 3.6, 2.7 and 2.2° and 0.164, 0.141, and 0.132 Å. The largest differences between the mean-square displacement amplitudes

---

[8]) This method of absorption correction, using only one φ profile, was successful with our crystal-mounting technique in several cases, *e.g.* [10]. Because the crystal is situated on the *side* of the glass fibre (made from *Lindemann* glass) and because it is covered with a drop of oil, it is practically impossible to determine the indices of the crystal faces so that all methods requiring the plane equations of the faces are not applicable (*e.g.* ABSORB or LSABS from the Xtal 3.2 [21] system).

of bonded atoms were −0.007(4) Å^2 for C(1)–C(6) and −0.006(4) Å^2 for C(4)–C(41). All rigid-body corrections of C–C bond lengths were less than 0.005 Å and thus negligible.

NMR Spectra of **1**·Sb_2F_{11} *(Dissolved Crystals).* The flask with the dry crystals was stored on dry ice for more than two weeks during which no significant decomposition was optically detectable by repeated microscopical investigation of crystal samples on the cryostage. Finally, after completion of the X-ray measurements, 1 ml of CD_2Cl_2 was slowly added at −80° to the dry crystals, and 0.5 ml of the supernatant yellow soln. was rapidly transferred under Ar into a cooled NMR tube. The NMR (^{1}H: 400 MHz; ^{13}C: 100 MHz) measurements were carried out at −81.0°. ^{1}H-NMR: 1.756 (very intense, br.); 2.031 (smaller, br.); several other sharp peaks (from hydrolysis or decomposition products which might be enriched in the soln. by washing of the crystals). ^{13}C-NMR: probably only signals from the (probably nonexchanging) decomposition products (low concentration of **1**·Sb_2F_{11}). The NMR spectra are shown in the *Supplementary Material* in figs. S22 and S23.

Supplementary Material. – Available from the author: Packing diagram; tables of positional and thermal parameters, bond distances, angles, torsion angles, interatomic distances; electron- and difference-density maps; NMR spectra; table of observed and calculated structure factors (72 pages). The numerical data of the *Supplementary Material* and the *CAD4* data and log files are also available as ASCII files.

This work was sponsored by the allocation of a 'Dozentenstipendium' of the *Fonds der Chemischen Industrie*, Federal Republic of Germany. I thank Mr. *Thomas Blatter* for the syntheses of isofenchone. The cryostage was built by Mr. *Kurt Baumgartner* and Mr. *Beat Huber*, workshop of the Laboratory of Organic Chemistry, who contributed many hints and ideas for the construction. The NMR spectra were recorded by Mrs. *Brigitte Brandenberg* and Mr. *Christian Lohse*. All computations were done on a *Sun SPARCserver 2* which was bought by the computer center of the ETH.

REFERENCES

[1] Reviews and monographs: C.A. Grob, *Acc. Chem. Res.* **1983,** *16,* 426; H.C. Brown, *ibid.* **1983,** *16,* 432; G.A. Olah, G.K.S. Prakash, M. Saunders, *ibid.* **1983,** *16,* 440; C. Walling, *ibid.* **1983,** *16,* 448; M. Saunders, H.A. Jiménez-Vázquez, *Chem. Rev.* **1991,** *91,* 375; P. Buzek, P.v.R. Schleyer, S. Sieber, *Chem. Unserer Zeit* **1992,** *26,* 116; H.C. Brown, 'The Nonclassical Ion Problem (with Comments by P.v.R. Schleyer)', Plenum Press, New York, 1977; G.A. Olah, G.K.S. Prakash, J. Sommer, 'Superacids', John Wiley & Sons, New York, 1985, pp. 132–142.

[2] a) G.A. Olah, G.K.S. Prakash, M. Arvanaghi, F.A.L. Anet, *J. Am. Chem. Soc.* **1982,** *104,* 7105; C.S. Yannoni, V. Macho, P.C. Myhre, *ibid.* **1982,** *104,* 907, 7380; P.C. Myhre, G.G. Webb, C.S. Yannoni, *ibid.* **1990,** *112,* 8991; b) W. Koch, B. Liu, D.J. DeFrees, D.E. Sunko, H. Vančik, *Angew. Chem.* **1990,** *102,* 198; *ibid. Int. Ed.* **1990,** *29,* 183; c) W. Koch, B. Liu, D.J. DeFrees, *J. Am. Chem. Soc.* **1989,** *111,* 1527.

[3] a) G.A. Olah, *Aldrichim. Acta* **1979,** *12,* 43; b) J.P. Dinnocenzo, Ph.D. Thesis, Cornell University, Ithaca, NY, 1985.

[4] a) T. Laube, *Angew. Chem.* **1987,** *99,* 580; *ibid. Int. Ed.* **1987,** *26,* 560; b) T. Laube, *J. Am. Chem. Soc.* **1989,** *111,* 9224; c) T. Laube, *Acta Crystallogr., Sect. A* **1992,** *48,* 158.

[5] L.K. Montgomery, M.P. Grendze, J.C. Huffman, *J. Am. Chem. Soc.* **1987,** *109,* 4749.

[6] G.A. Olah, J.R. DeMember, C.Y. Lui, R.D. Porter, *J. Am. Chem. Soc.* **1971,** *93,* 1442; M. Saunders, L. Telkowski, M.R. Kates, *ibid.* **1977,** *99,* 8070; P.C. Myhre, K.L. McLaren, C.S. Yannoni, *ibid.* **1985,** *107,* 5294.

[7] J.M. Coxon, P.J. Steel, *Aust. J. Chem.* **1979,** *32,* 2441.

[8] G.A. Olah, J.T. Welch, Y.D. Vankar, M. Nojima, I. Kerekes, J.A. Olah, *J. Org. Chem.* **1979,** *44,* 3872.

[9] L. Huang, K. Ranganayakulu, T.S. Sorensen, *J. Am. Chem. Soc.* **1973,** *95,* 1936.

[10] S. Hollenstein, T. Laube, *J. Am. Chem. Soc.* **1993,** *115,* 7240.

[11] C.K. Johnson, C.J. Collins, *J. Am. Chem. Soc.* **1974,** *96,* 2514.

[12] L. Doms, D. Van Hemelrijk, W. Van de Mieroop, A.T.H. Lenstra, H.J. Geise, *Acta Crystallogr., Sect. B* **1985,** *41,* 270; A.N. Fitch, H. Jobic, *J. Chem. Soc., Chem. Commun.* **1993,** 1516.

[13] F.H. Allen, O. Kennard, D.G. Watson, L. Brammer, A.G. Orpen, R. Taylor, in 'International Tables for Crystallography, Volume C', Ed. A.J.C. Wilson, Kluwer Academic Publishers, Dordrecht, 1992, pp. 685–706.

[14] R. Haseltine, K. Ranganayakulu, N. Wong, T.S. Sorensen, *Can. J. Chem.* **1975,** *53,* 1901; T.S. Sorensen, *Acc. Chem. Res.* **1976,** *9,* 257.

[15] R. S. Krishnan, R. Srinivasan, S. Devanarayanan, 'Thermal Expansion of Crystals', Pergamon, Oxford, 1979, pp. 50–53.
[16] M. Veith, W. Frank, *Chem. Rev.* **1988,** *88,* 81.
[17] T. Kottke, D. Stalke, *J. Appl. Cryst.* **1993,** *26,* 615.
[18] H. Hope, *Acta Crystallogr., Sect. B* **1988,** *44,* 22.
[19] T. Laube, fotoplot, ETH Zürich, 1992.
[20] J. Stewart, R. Merom, J. Holden, R. Doherty, S. Hall, T. Maslen, N. Spadaccini, in 'DIFDAT. Xtal 3.2 Reference Manual', Eds. S. R. Hall, H. D. Flack, and J. M. Stewart, Universities of Western Australia, Geneva, and Maryland, Lamb, Perth, Australia, 1992, pp. 104–110.
[21] 'Xtal 3.2 Reference Manual', Eds. S. R. Hall, H. D. Flack, and J. M. Stewart, Universities of Western Australia, Geneva, and Maryland, Lamb, Perth, Australia, 1992; the program version used here contains the August 1993 updates.
[22] K. Watenpaugh, J. Stewart, 'ABSCAL. Xtal 3.2 Reference Manual', Eds. S. R. Hall, H. D. Flack, and J. M. Stewart, Universities of Western Australia, Geneva, and Maryland, Lamb, Perth, Australia, 1992, pp. 41–43.
[23] G. M. Sheldrick, 'SHELXS-86', University of Göttingen, 1986; G. M. Sheldrick, *Acta Crystallogr., Sect. A* **1990,** *46,* 467.
[24] G. M. Sheldrick, 'SHELXL-93', University of Göttingen, 1993; G. M. Sheldrick, *J. Appl. Cryst.* **1994,** in preparation.
[25] S. Hall, 'LISTFC. Xtal 3.2 Reference Manual', Eds. S. R. Hall, H. D. Flack, and J. M. Stewart, Universities of Western Australia, Geneva, and Maryland, Lamb, Perth, Australia, 1992, pp. 153–155.
[26] R. Olthof-Hazekamp, 'CRYLSQ. Xtal 3.2 Reference Manual', Eds. S. R. Hall, H. D. Flack, and J. M. Stewart, Universities of Western Australia, Geneva, and Maryland, Lamb, Perth, Australia, 1992, pp. 93–103.
[27] P. J. Becker, P. Coppens, *Acta Crystallogr., Sect. A* **1974,** *30,* 148.
[28] J. Stewart, J. Holden, R. Doherty, S. Hall, 'FOURR. Xtal 3.2 Reference Manual', Eds. S. R. Hall, H. D. Flack, and J. M. Stewart, Universities of Western Australia, Geneva, and Maryland, Lamb, Perth, Australia, 1992, pp. 118–124.
[29] N. Spadaccini, R. Alden, 'SLANT. Xtal 3.2 Reference Manual', Eds. S. R. Hall, H. D. Flack, and J. M. Stewart, Universities of Western Australia, Geneva, and Maryland, Lamb, Perth, Australia, 1992, pp. 303–306.
[30] M. Spackman, 'CONTRS. Xtal 3.2 Reference Manual', Eds. S. R. Hall, H. D. Flack, and J. M. Stewart, Universities of Western Australia, Geneva, and Maryland, Lamb, Perth, Australia, 1992, pp. 82–87.
[31] V. Streltsov, 'PREVUE. Described in: Notes from Ozy', Eds. S. R. Hall, H. D. Flack, and J. M. Stewart, Universities of Western Australia, Geneva, and Maryland, Vol. III, No. 8, August 1993.
[32] S. Hall, R. Olthof-Hazekamp, H. Flack, J. Hester, U. Bartsch, 'PLOTX. Xtal 3.2 Reference Manual', Eds. S. R. Hall, H. D. Flack, and J. M. Stewart, Universities of Western Australia, Geneva, and Maryland, Lamb, Perth, Australia, 1992, pp. 244–246.
[33] S. Hall, R. Doherty, 'PEKPIK. Xtal 3.2 Reference Manual', Eds. S. R. Hall, H. D. Flack, and J. M. Stewart, Universities of Western Australia, Geneva, and Maryland, Lamb, Perth, Australia, 1992, pp. 232–234.
[34] G. Davenport, S. Hall, W. Dreissig, 'ORTEP. Xtal 3.2 Reference Manual', Eds. S. R. Hall, H. D. Flack, and J. M. Stewart, Universities of Western Australia, Geneva, and Maryland, Lamb, Perth, Australia, 1992, pp. 219–224; original version: C. K. Johnson, 'ORTEP-II', Oak Ridge National Laboratory, TN 37830, 1976.
[35] '*SYBYL*® Version 6.0 for Sun Computers'[9]), November 1992, *Tripos Associates, Inc.* (a subsidiary of *Evans & Sutherland*), St. Louis, MO 63144-2913.
[36] M. Nardelli, 'PARST88, Release April 1988', University of Parma, Italy; M. Nardelli, *Comp. Chem.* **1983,** *7,* 95.
[37] K. Trueblood, 'THMA11, Version of Oct. 21, 1988', University of California, Los Angeles, CA 90024.

[9]) The programs res2dat, dat2cry and cry2mol (T. Laube, ETH Zürich, 1993) were used for the conversion of coordinate files in various formats to files in the 'mol' format which were read by *SYBYL* and then processed interactively. The generated *PostScript* files require some editing concerning the atom labels.